Response to review #2

We thank the reviewer for the constructive comments and suggestions, which are very positive to improve scientific content of the manuscript. We have revised the manuscript appropriately and addressed all the reviewer's comments point-by-point for consideration as below. The remarks from the reviewer are shown in black, and our responses are shown in blue color. All the page and line numbers mentioned following are refer to the revised manuscript without change tracked.

This study examined long-term HCHO columns in Shanghai with OMI and ground-based remote sensing observations. The author also studied the ozone sensitivity in Shanghai and proposed a correction factor to satellite HCHO to NO2 ratio. The authors found that applying such a correction results in ozone formation is more likely to be under the VOC-limited regime. In my view, this work is among few studies exclusively focusing on HCHO observations and ozone sensitivity in China, thus is appropriate for publication at ACP subject to the following concerns.

1. The authors examined monthly averaged columns at a spatial resolution of 0.01°×0.01° degree. I am not sure whether there would be enough pixels in each grid cell to reduce the uncertainty in mean HCHO column to a much lower and acceptable level. This could be a potential issue in the winter seasons when SZA is high and the light path is long.

R: Thanks for your professional comments. In order to check whether there were enough pixels in each grid, we have counted the number of days that each grid has been assigned with HCHO VCDs between 2010 and 2019 on monthly scale. Here, we have defined the effective observation days (EODs) as the number of days that once any grid within Shanghai areas has been still designated after the data quality filtering. Afterwards, we have calculated the percentages of areas with observed days reached 60% EODs for every month during 2010-2019, results are shown in Table R1. For example, in January, about 80% areas of Shanghai have been assigned with HCHO VCDs during more than 60% of the total EODs.

Table R1. Proportion of areas with observed days reached 60% EODs in each month of 2010-2019.

Month	Proportion	Month	Proportion
January	79.9% ± 24.6%	July	72.2% ± 31.8%
February	61.6% ± 33.6%	August	69.7% ± 25.7%
March	87.7% ± 16.5%	September	71.2% ± 33.4%
April	94.3% ± 9.1%	October	59.7% ± 30.9%
May	86.1% ± 30.2%	November	88.5% ± 13.3%
June	33.4% ± 25.1%	December	84.4% ± 18.6%

Table R1 reveals that the winter months did not show the obvious low proportion, while the proportion in June is much lower. It can be explained by the impacts of abundant precipitation in June (as shown in Figure S2), which leads to only a small amount of areas were assigned with HCHO VCD on the EOD after screening by cloud fraction. So, we considered that the monthly averaged HCHO VCDs can be the representative of the mean level of HCHO in Shanghai when the temporal patterns were discussed in the manuscript. While the spatial characteristics have been investigated with high spatial resolution only when more EODs have been oversampled, e.g. in seasonal with multiple years averaged.

2. Did the authors correct the well-known drift in OMI SAO HCHO product? If not, please do so and update the results accordingly.

R: Thanks for your suggestions. Previous studies mentioned that OMI-SAO HCHO columns display significant drift due to instrument aging (Marais et al., 2012; Zhu et al., 2014; Zhu et al., 2017), in which OMI HCHO Version 2.0 data were used. However, the updated product (OMI HCHO Version 3.0) were used in this study, which has a significant improvement in treating the increasing trend of background values (https://aura.gesdisc.eosdis.nasa.gov/data/Aura_OMI_Level2/OMHCHO.003/doc/README.OMHCHO.pdf).

In order to check whether there is still obvious drift, we have performed temporal linear regression of the deseasonalized monthly averaged HCHO columns during 2010-2019 for remote pacific region (29°-33°N, 160°-140°W) around the same latitude as Shanghai (Zhu et al., 2017). Zonal mean HCHO columns have been calculated with 0.5° latitude steps. It was found that there was no obvious linear trend for the deseasonalized HCHO VCDs on monthly scale in those eight zonal latitude ranges (R^2 ranged from 0.06 to 0.19 with average of 0.11), suggesting that the updated OMI HCHO product used in this study does not include the obvious drift. Figure R2 shows the time series of deseasonalized zonal mean HCHO VCDs for the highest and lowest latitudes on monthly scale. We have clarified in the manuscript, please refer to Line 99-101.

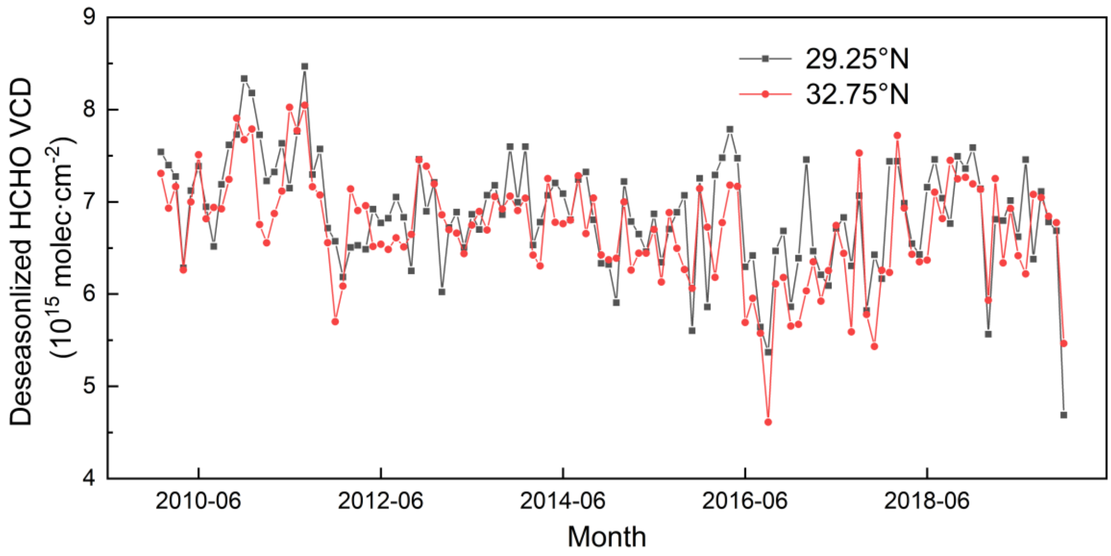

Figure R2. The time series of deseasonalized zonal monthly mean HCHO VCDs of different latitudes in the remote pacific region (29°-33°N, 160°-140°W). Monthly variations of zonal mean

HCHO VCD with the maximum and minimum latitude are exhibited as the example (29.25°N and 32.75°N stands for range of 29.0°-29.5°N and 32.5°-33.0°N, respectively).

3. In page 7, please clarify how to get the HCHO emission rate? Is HCHO mainly secondary? If so, how to determine HCHO yields from NMVOCs? The authors may also want to consider the lower HCHO yields from NMVOCs as NOx emissions drop in the study period.

R: Thank you for the professional comments. Figure 7 in the original manuscript reflects the annual anthropogenic HCHO primary emissions and does not include the secondary production of HCHO. However, secondary production of HCHO from anthropogenic and biogenic sources has contributed greatly to HCHO (Zhu et al., 2017; Shen et al., 2019). As suggested by Reviewer #1, we have also considered the secondary production of HCHO in the revised manuscript, including anthropogenic and biogenic sources. Please refer to Line 176-205.

In order to get the secondary production of HCHO from anthropogenic sources, Non-methane volatile organic compounds (NMVOCs) emission inventory based on the SAPRC07 mechanism species from Multi-resolution Emission Inventory for China (MEIC) was used for years of 2010, 2012, 2014 and 2016. Secondary production of HCHO has been calculated based on 1-day HCHO yields of several NMVOCs under high-NO_x condition (Shen et al., 2019). Table R2 summarizes the primary emissions and secondary productions of HCHO from different sectors of anthropogenic sources.

Table R2. The primary emissions and estimated secondary productions of HCHO in Shanghai from anthropogenic NMVOCs based on SAPRC07 mechanism species.

Year		Estimated HCHO production from each sector (10^9 g)				
		Industry	Power	Residential	Transportation	Total
2010	Primary[1]	9.10	0.03	0.06	1.47	10.66
	Secondary[2]	240.58	0.52	15.14	66.04	322.28
2012	Primary	7.73	0.05	0.07	1.01	8.86
	Secondary	246.67	0.57	15.67	51.91	314.82
2014	Primary	6.88	0.05	0.07	0.74	7.74
	Secondary	253.32	0.50	16.44	44.32	314.58
2016	Primary	6.29	0.05	0.06	0.61	7.01
	Secondary	286.36	0.51	16.64	43.14	346.65

[1] Primary indicates HCHO that is directly emitted by anthropogenic sources from MEIC inventory.

[2] Secondary indicates HCHO that is produced by anthropogenic NMVOCs, which is calculated based on 1-day HCHO yields.

Regardless of the primary emissions or secondary productions of HCHO, industry sector corresponds to the largest yield, followed by transportation, residential, and the power. For the temporal trend, the primary emission of HCHO keeps decreasing (about 34.2% compared to 2010), while secondary produced HCHO did not change significantly. The increase of secondary HCHO yields in 2016 was mainly due to the increased production from industry sector. In addition, the changes and proportional relationships between primary emission and secondary production of HCHO for different sectors are different, which suggests the VOCs source profiles of different sectors would affect the amount of secondary HCHO production.

HCHO yield from biogenic sources can be estimated from BVOCs emission inventory. Model of Emissions of Gases and Aerosols from Nature (MEGAN) is widely used to simulate the emission of BVOCs. As we currently cannot use MEGAN to accurately simulate four-year (2010, 2012, 2014, 2016) BVOCs emissions, we have used the annual total BVOCs emissions of Shanghai in 2014 (about 1.2×10^4 t) for the estimation (Liu et al., 2018a; Liu et al., 2018b). Isoprene, methanol and monoterpenes were dominant compositions of BVOCs and accounted about 81.3% of the total. We have calculated HCHO yields contributed by isoprene, methanol and monoterpenes, as shown in Table R3.

Table R3. The annual BVOCs emissions and HCHO yields over Shanghai in 2014.

BVOC	Emission (10^9 g)	HCHO yield (10^9 g)
Isoprene	4.63	4.70
Methanol	4.26	3.99
Monoterpenes	0.86	0.38
Total	9.75	9.07

Accordingly, HCHO yield from BVOCs emission was estimated to be about 9.07×10^9 g, and mostly produced from isoprene and methanol. The calculated HCHO yield from BVOCs emission is similar to that of previous study during 2005-2016 (Shen et al., 2019). In addition, compared with anthropogenic sources, HCHO yield from BVOCs is much smaller, which indicates that the anthropogenic is the main contributor of secondary production of HCHO in Shanghai (Shen et al., 2019; Fan et al., 2021).

As shown in Table R4, we have also reviewed the related studies about the BVOCs emissions in Shanghai and its surrounding areas (the Yangtze River Delta) in relevant years. Wang et al. (2021a) assessed the impacts of land cover change and climate variability on BVOCs emissions in China from 2001 to 2016, in which variations of BVOCs emissions in Shanghai over the years were extremely small. Considering the different input dataset and settings would bring large differences in the simulated results, it was unfeasible to use BVOCs emissions from different studies for the investigation of temporal variation. Therefore, the BVOCs emissions in 2014 were used to basically characterize the approximate level of BVOCs from 2010 to 2016 in this study.

Table R4. Comparison of simulated BVOCs emissions in Shanghai (SH) and the Yangtze River Delta (YRD) based on MEGAN.

Simulated year	Reference	MEGAN version	Region	BVOCs emission (10^4 t)
2010	Song et al. (2012)[1]	V 2.04	YRD	110
			SH	0.122
2014	Liu et al. (2018a; 2018b)[2]	V 2.10	YRD	188.6
			SH	1.2
2016	Wang et al. (2021b)[3]	V 3.1	YRD	162 [1]
			SH	~ 0.34 [4]

[1] Total annual emission inferred from the simulated BVOCs emissions in January, April, July and October.

[2] A variety of methods were used to reduce the uncertainty of plant functional types (PFT) database. The proportions of dominant components of BVOCs were also provided.

[3] BVOCs emission was simulated without drought stress.

[4] It is BVOCs emissions in July, which has been inferred from Fig. S3 of Wang et al. (2021b).

In addition, it should be noted that HCHO yield was also impacted by the NO_x levels, e.g. RO_2 radical from VOCs react with HO_2 to from organic peroxides under low NO_x condition. This process reduces the reaction of RO_2 and NO, which in turn decreases the production of HCHO, therefore, HCHO yield from VOCs is proportional to NO_x condition (Palmer et al., 2006; Marais et al., 2012; Miller et al., 2017). In this study, the estimation using a fixed HCHO yield may overestimate HCHO production in later years due to the decreases of NO_x in Shanghai (Xue et al., 2020). In previous studies, the proportional relationship between HCHO yield and NO_x condition was usually obtained when 1 ppbv of NO_x regard as the high condition, and 0.1 ppbv of NO_x regard as low condition (Palmer et al., 2006; Marais et al., 2012; Miller et al., 2017). However, the NO_x concentration in Shanghai is still relatively higher (basically 30-60 ppbv in urban) (Gao et al., 2017). Therefore, in such a high NO_x condition, the effect of NO_x decreases on HCHO yield needs to be further studied.

Minor comments:

1. Page 2, line 39-40, please include GOME-2 A, B, and C

R: Thanks for the suggestion. We have added GOME-2 A, B, and C in the Introduction, please refer to Line 39.

2. Page 3, line 76, please change “in a day” to “in the daytime”

R: We have corrected ‘in a day’ to ‘in the daytime’. Please refer to Line 76.

3. Page 3, line 80, please change “pixels” to “rows”

R: We have corrected ‘pixels’ to ‘rows’. Please refer to Line 80.

4. Page 3, line 81, here and elsewhere, please change “~” to “-”. “~” means “approximately”

R: Thanks for the reminding. We have changed ‘~’ to ‘-’. Please refer to Line 81.

5. Page 3, line 92-93, I think by using MainQualityFlag=0 as the criterion, you have filtered out pixels affected by row anomalies already.

R: Thanks for your comments. Pixels flagged with 0 in field MainDataQualityFlag were considered to be passed quality check. However, in OMHCHO V3.0 product, field XtrackQualityFlags has been carried over from the L1b product to characterize pixels affected by the row anomaly. We have tested and found that the usage of XtrackQualityFlags during the filtering process can affect the results. As shown in Figure R3, under the two filtering conditions, HCHO VCDs have obvious differences in some regions. In addition, Figure R3(a) exists a track with abnormally high value, which basically disappeared after being filtered by using XtrackQualityFlags. It means that including XtrackQualityFlags in filtering criterion in addition to MainDataQualityFlag would be effective.

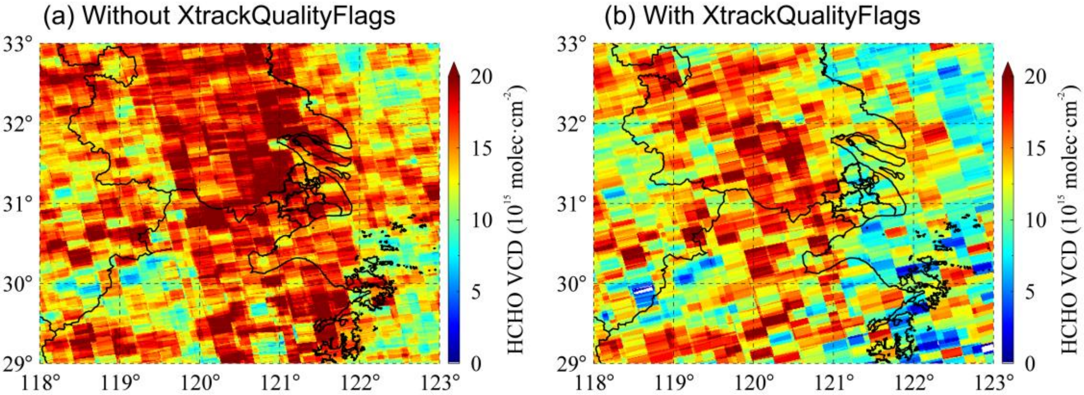

Figure R3. Spatial distribution of HCHO VCDs of Shanghai and surrounding areas in October 2010 under different filter conditions of (a) without XtrackQualityFlags and (b) with XtrackQualityFlags.

6. Page 5, line 127-129, could you please explain the spatial variations in HCHO columns. Is the spatial pattern consistent with emissions?

R: Thanks for your comments. For determining whether the spatial variations in HCHO VCD is consistent with local emissions, we have displayed the spatial distribution of anthropogenic NMVOCs in Shanghai in 2017 with high resolution of 4 km×4 km in Figure R4 (An et al., 2021). It can be seen that the hotspots of NMVOCs emission were concentrated in the city center, while the highest HCHO VCD appeared in the relatively remote Qingpu district, where the NMVOCs emissions were relatively low. Obviously, the anthropogenic emissions and HCHO VCD do not coincide well in the spatial pattern, and the high value of HCHO VCD in Qingpu district cannot be directly explained by the emission of anthropogenic NMVOCs.

Not only high HCHO VCD observed by satellites, but also high concentrations of surface HCHO have been measured in Qingpu District (e.g. Su et al., 2019; Zhang et al., 2021). Impact of air masses transport containing high concentrations of reactive VOCs from adjacent Zhejiang Province and Jiangsu Province was reported (Zhang et al., 2020). As shown in Figure R4, the anthropogenic NMVOCs inventory in the Yangtze River Delta also displays that there were obvious sources of NMVOCs in the southern part of Jiangsu and the northern part of Zhejiang. The high local atmospheric oxidation capacity leads to the rapid degradation of VOCs, which in turn enhances the contributions of anthropogenic NMVOCs to the local HCHO production in Qingpu district (Zhang et al., 2021).

In addition, model simulation showed that isoprene plays an important role in the production of HCHO as the precursor, and it can contribute about 36% of the production of HCHO during O_3 formation episodes from April to June in 2018 in Qingpu district (Zhang et al., 2021). The abundant BVOCs in Qingpu district may be another important reason for the high HCHO VCD. Please refer to Line 139-143.

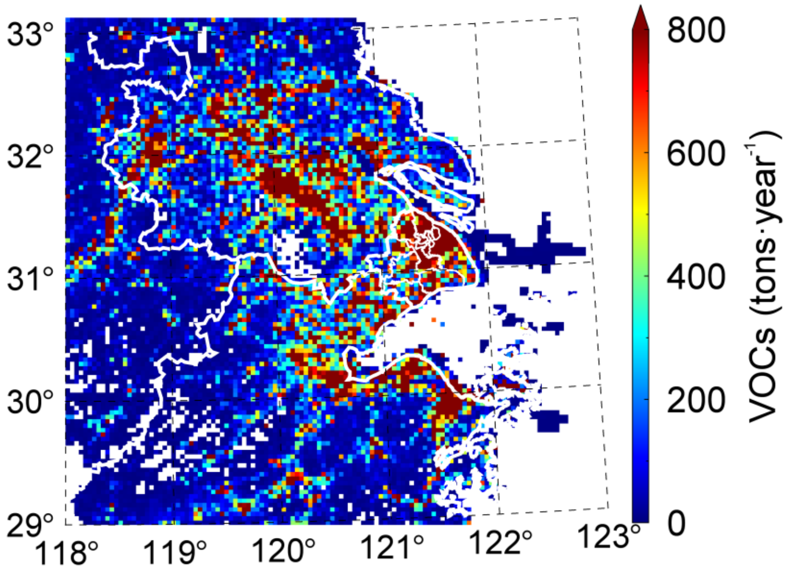

Figure R4. Anthropogenic NMVOCs emissions in Shanghai in 2017. The inventory data is available from An et al. (2021).

Reference:

An, J. Y., Huang, Y. W., Huang, C., Wang, X., Yan, R. S., Wang, Q., Wang, H. L., Jing, S. A., Zhang, Y., Liu, Y. M., Chen, Y., Xu, C., Qiao, L. P., Zhou, M., Zhu, S. H., Hu, Q. Y., Lu, J., and Chen, C. H.: Emission inventory of air pollutants and chemical speciation for specific anthropogenic sources based on local measurements in the Yangtze River Delta region, China, Atmos Chem Phys, 21, 2003-2025, https://doi.org/10.5194/acp-21-2003-2021, 2021.

Fan, J. C., Ju, T. Z., Wang, Q. H., Gao, H. Y., Huang, R. R., and Duan, J. L.: Spatiotemporal variations and potential sources of tropospheric formaldehyde over eastern China based on OMI satellite data, Atmos Pollut Res, 12, 272-285, https://doi.org/10.1016/j.apr.2020.09.011, 2021.

Gao, W., Tie, X. X., Xu, J. M., Huang, R. J., Mao, X. Q., Zhou, G. Q., and Chang, L. Y.: Long-term trend of O-3 in a mega City (Shanghai), China: Characteristics, causes, and interactions with precursors, Sci Total Environ, 603, 425-433, https://doi.org/10.1016/j.scitotenv.2017.06.099, 2017.

Liu, Y., Li, L., An, J., Zhang, W., Yan, R., Huang, L., Huang, C., Wang, H., Wang, Q., and Wang, M.:

Emissions, Chemical Composition, and Spatial and Temporal Allocation of the BVOCs in the Yangtze River Delta Region in 2014, ENVIRONMENTAL SCIENCE, 39, 608-617, 2018a.
Liu, Y., Li, L., An, J. Y., Huang, L., Yan, R. S., Huang, C., Wang, H. L., Wang, Q., Wang, M., and Zhang, W.: Estimation of biogenic VOC emissions and its impact on ozone formation over the Yangtze River Delta region, China, Atmos Environ, 186, 113-128, https://doi.org/10.1016/j.atmosenv.2018.05.027, 2018b.
Marais, E. A., Jacob, D. J., Kurosu, T. P., Chance, K., Murphy, J. G., Reeves, C., Mills, G., Casadio, S., Millet, D. B., Barkley, M. P., Paulot, F., and Mao, J.: Isoprene emissions in Africa inferred from OMI observations of formaldehyde columns, Atmos Chem Phys, 12, 6219-6235, https://doi.org/10.5194/acp-12-6219-2012, 2012.
Miller, C. C., Jacob, D. J., Marais, E. A., Yu, K. R., Travis, K. R., Kim, P. S., Fisher, J. A., Zhu, L., Wolfe, G. M., Hanisco, T. F., Keutsch, F. N., Kaiser, J., Min, K. E., Brown, S. S., Washenfelder, R. A., Abad, G. G., and Chance, K.: Glyoxal yield from isoprene oxidation and relation to formaldehyde: chemical mechanism, constraints from SENEX aircraft observations, and interpretation of OMI satellite data, Atmos Chem Phys, 17, 8725-8738, https://doi.org/10.5194/acp-17-8725-2017, 2017.
Palmer, P. I., Abbot, D. S., Fu, T. M., Jacob, D. J., Chance, K., Kurosu, T. P., Guenther, A., Wiedinmyer, C., Stanton, J. C., Pilling, M. J., Pressley, S. N., Lamb, B., and Sumner, A. L.: Quantifying the seasonal and interannual variability of North American isoprene emissions using satellite observations of the formaldehyde column, J. Geophys. Res.-Atmos., 111, 14, https://doi.org/10.1029/2005jd006689, 2006.
Shen, L., Jacob, D. J., Zhu, L., Zhang, Q., Zheng, B., Sulprizio, M. P., Li, K., De Smedt, I., Abad, G. G., Cao, H. S., Fu, T. M., and Liao, H.: The 2005-2016 Trends of Formaldehyde Columns Over China Observed by Satellites: Increasing Anthropogenic Emissions of Volatile Organic Compounds and Decreasing Agricultural Fire Emissions, Geophys Res Lett, 46, 4468-4475, https://doi.org/10.1029/2019gl082172, 2019.
Song, Y., Zhang, Y., Wang, Q., and An, J.: Estimation of biogenic VOCs emissions in Eastern China based on remote sensing data, Acta Sci Circum, 32, 2216-2227, 2012.
Su, W. J., Liu, C., Hu, Q. H., Zhao, S. H., Sun, Y. W., Wang, W., Zhu, Y. Z., Liu, J. G., and Kim, J.: Primary and secondary sources of ambient formaldehyde in the Yangtze River Delta based on Ozone Mapping and Profiler Suite (OMPS) observations, Atmos Chem Phys, 19, 6717-6736, https://doi.org/10.5194/acp-19-6717-2019, 2019.
Wang, H., Wu, Q. Z., Guenther, A. B., Yang, X. C., Wang, L. N., Xiao, T., Li, J., Feng, J. M., Xu, Q., and Cheng, H. Q.: A long-term estimation of biogenic volatile organic compound (BVOC) emission in China from 2001-2016: the roles of land cover change and climate variability, Atmos Chem Phys, 21, 4825-4848, https://doi.org/10.5194/acp-21-4825-2021, 2021a.
Wang, Y. J., Tan, X. J., Huang, L., Wang, Q., Li, H. L., Zhang, H. Y., Zhang, K., Liu, Z. Y., Traore, D., Yaluk, E., Fu, J. S., and Li, L.: The impact of biogenic emissions on ozone formation in the Yangtze River Delta region based on MEGANv3.1, Air Qual. Atmos. Health, 14, 763-774, https://doi.org/10.1007/s11869-021-00977-0, 2021b.
Xue, R. B., Wang, S. S., Li, D. R., Zou, Z., Chan, K. L., Valks, P., Saiz-Lopez, A., and Zhou, B.: Spatio-temporal variations in NO_2 and SO_2 over Shanghai and Chongming Eco-Island measured by Ozone Monitoring Instrument (OMI) during 2008-2017, J Clean Prod, 258, 14, https://doi.org/10.1016/j.jclepro.2020.120563, 2020.
Zhang, K., Li, L., Huang, L., Wang, Y. J., Huo, J. T., Duan, Y. S., Wang, Y. H., and Fu, Q. Y.: The impact of volatile organic compounds on ozone formation in the suburban area of Shanghai, Atmos Environ,

232, 11, https://doi.org/10.1016/j.atmosenv.2020.117511, 2020.
Zhang, K., Huang, L., Li, Q., Huo, J. T., Duan, Y. S., Wang, Y. H., Yaluk, E., Wang, Y. J., Fu, Q. Y., and Li, L.: Explicit modeling of isoprene chemical processing in polluted air masses in suburban areas of the Yangtze River Delta region: radical cycling and formation of ozone and formaldehyde, Atmos Chem Phys, 21, 5905-5917, https://doi.org/10.5194/acp-21-5905-2021, 2021.
Zhu, L., Jacob, D. J., Mickley, L. J., Marais, E. A., Cohan, D. S., Yoshida, Y., Duncan, B. N., Abad, G. G., and Chance, K. V.: Anthropogenic emissions of highly reactive volatile organic compounds in eastern Texas inferred from oversampling of satellite (OMI) measurements of HCHO columns, Environ Res Lett, 9, 7, https://doi.org/10.1088/1748-9326/9/11/114004, 2014.
Zhu, L., Mickley, L. J., Jacob, D. J., Marais, E. A., Sheng, J. X., Hu, L., Abad, G. G., and Chance, K.: Long-term (2005-2014) trends in formaldehyde (HCHO) columns across North America as seen by the OMI satellite instrument: Evidence of changing emissions of volatile organic compounds, Geophys Res Lett, 44, 7079-7086, https://doi.org/10.1002/2017gl073859, 2017.